

Studies of a reversed field pinch in a poloidal divertor configuration

This article has been downloaded from IOPscience. Please scroll down to see the full text article.

1989 Nucl. Fusion 29 104

(<http://iopscience.iop.org/0029-5515/29/1/014>)

View [the table of contents for this issue](#), or go to the [journal homepage](#) for more

Download details:

IP Address: 128.104.165.254

The article was downloaded on 07/02/2011 at 20:49

Please note that [terms and conditions apply](#).

STUDIES OF A REVERSED FIELD PINCH IN A POLOIDAL DIVERTOR CONFIGURATION

J.S. SARFF, A.F. ALMAGRI, S. ASSADI,
D.J. DEN HARTOG, R.N. DEXTER,
S.C. PRAGER, J.C. SPROTT (Department of Physics,
University of Wisconsin-Madison, Madison, Wisconsin,
United States of America)

ABSTRACT. An attempt has been made to form a reversed field pinch (RFP) in a poloidal divertor configuration which positions the plasma far from a conducting wall. In this configuration, the plasma is localized within a magnetic separatrix formed by a combination of toroidal currents in the plasma and four internal aluminium rings. Plasmas were formed with a plasma current of ~ 135 kA, toroidal field reversal lasting ~ 1 ms, line averaged density of $\sim (1-2) \times 10^{13}$ cm^{-3} and central electron temperature of ~ 50 eV, but a large asymmetry in the magnetic field ($\delta B/B \sim 40\%$) set in at about the time when the toroidal field reversed at the wall. This behaviour might be expected on the basis of MHD stability analysis of a cylindrical plasma bounded by a large vacuum region and a distant conducting wall. The symmetric equilibrium before the asymmetry develops and the asymmetry itself are described.

1. INTRODUCTION

Most reversed field pinch (RFP) experiments are performed in circular cross-section devices with close fitting conducting walls [1]. Linear magnetohydrodynamic (MHD) calculations predict that a conducting wall is required to stabilize current driven modes in an RFP, although a thin vacuum region between the plasma and the wall is allowed [2, 3]. The effect of a close fitting resistive shell RFP boundary is currently a central RFP physics issue, under investigation both theoretically and experimentally [4-6]. An RFP bounded by a large vacuum region is being studied theoretically, both linearly [7] and non-linearly [8], while experiments are planned for MST [9], the new RFP device at the University of Wisconsin, to investigate such a configuration.

In this letter we present the results of attempts to form a four-node poloidal divertor RFP. In this configuration, shown in Fig. 1, a magnetic separatrix is formed which acts to limit magnetically the plasma current and pressure. Internal equilibrium measurements in a similar device, Tokapole II, show this limiting action to be effective [10]. If the tenuous plasma region outside the separatrix is 'vacuum-like',

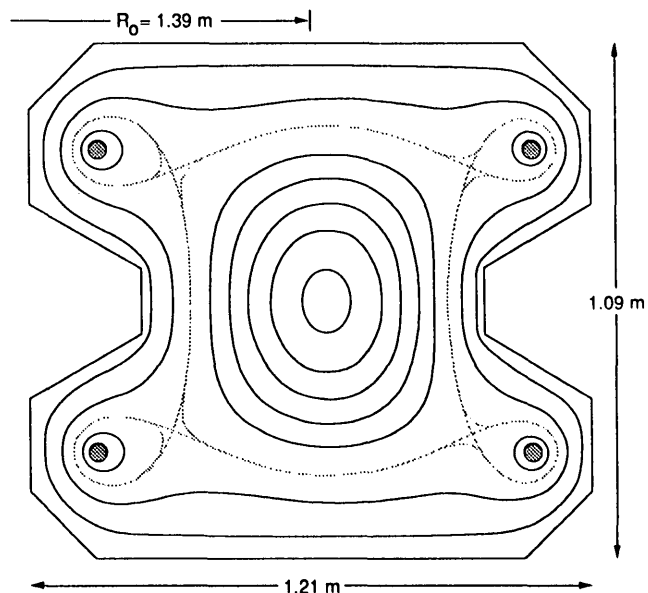


FIG. 1. Numerically computed plot of the equilibrium poloidal magnetic flux for the four-node poloidal divertor configuration with a plasma current equal to 60% of the total ring current. The broken contour is the magnetic separatrix.

then an RFP formed within the separatrix is located far from the stabilizing wall. Although stability calculations for these equilibria have not been performed, a variety of unstable modes is predicted in a cylindrical RFP when an equivalent vacuum region is included [7]. Indeed, it was observed that the plasma developed a large, stationary asymmetry at about the time when the toroidal field reversed at the wall. This asymmetry had dominantly an $m = 1$ poloidal mode number and large toroidal mode numbers (~ 5).

The usual emphasis in divertor configuration experiments is on controlling the plasma boundary as envisioned in a fusion reactor and on understanding the concomitant changes in the bulk plasma. The focus of our experiment is the behaviour of an RFP plasma far from a conducting wall. Other RFP-like devices, OHTE [11] and Multipinch [12], have operated with internal magnetic separatrices, but the effective 'vacuum' region in these devices was thought to be small enough to ensure ideal, linear MHD stability.

2. DEVICE DESCRIPTION AND DISCHARGE CHARACTERISTICS

The divertor configuration was formed by placing four aluminium rings of 4.13 cm minor diameter within an aluminium vacuum vessel of 1.39 m major radius

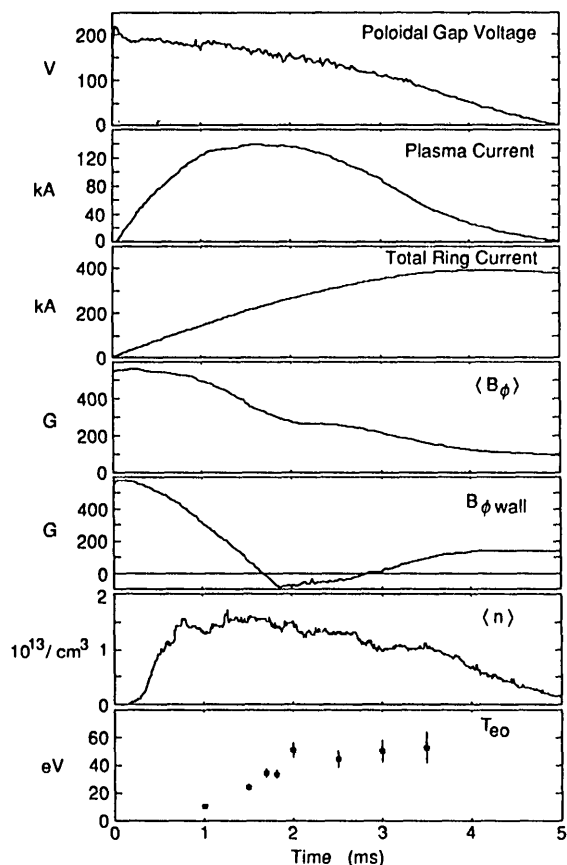


FIG. 2. Time evolution of electrical quantities, central-chord line averaged density and central electron temperature for a typical poloidal divertor RFP plasma. B_ϕ is the toroidal component of the magnetic field.

and 0.56 m average minor radius. These rings were located near force-free positions created by the wall indentations on the midplane and were rigidly suspended by 6.35 mm diameter Inconel rods attached to the wall; totals of 12 and 16 rods supported each inner and outer ring respectively.

The 5.0 cm thick aluminium wall served multiple functions as vacuum liner, toroidal and equilibrium field coils, and stabilizing conducting wall. The toroidal field was produced by a wall current fed from 44 pairs of leads connected across the single toroidal insulated gap (i.e. cut the long way around) and uniformly distributed in the toroidal direction. The poloidal field was generated by currents induced in the four rings and the plasma by a 12 turn primary winding on a 2.0 V·s iron core.

The time evolution of the basic electrical quantities, the line averaged density of the central chord and the central electron temperature for a typical 135 kA divertor RFP discharge is shown in Fig. 2. The density

was measured by a 140 GHz microwave interferometer, and the central electron temperature was measured by a single-point Thomson scattering system. A cw microwave source of ~ 2 kW at 2.45 GHz helped start up the plasma current by preionizing the H_2 fill gas. As the poloidal field increased, the toroidal field at the edge was programmed to reverse by ringing the wall current through zero and crowbaring it at a low negative value. Similar programming is used routinely in other RFP experiments [1]. The toroidal field remained reversed at the wall for ~ 1.2 ms while the average toroidal field, measured by a flux loop located just inside the wall, remained non-reversed.

To obtain radial profiles of the magnetic field, several probes were inserted on the midplane at toroidal azimuths of $\phi = 45^\circ$, $\phi = 135^\circ$ and $\phi = 225^\circ$ relative to the poloidal gap. The discharges examined were similar to the one described by Fig. 2; no appreciable change in these global quantities was observed with the probes inserted into the plasma. A typical probe consisted of a set of three small orthogonal magnetic pickup coils wound on a ceramic form and placed in a 0.127 mm thick, 4.76 mm diameter stainless steel tube covered by a 1.58 mm thick boron nitride heat shield. The coil signals were actively integrated to obtain the local magnetic field. To form a measurement of the equilibrium magnetic field, the probes were located at the same midplane radius and the components measured at the three azimuths were averaged. Also, the data from several shots were averaged to reduce shot-to-shot irregularities. The results at 1.6 ms ($\sim 150 \mu\text{s}$ before toroidal field reversal at the wall) for the toroidal and poloidal (vertical) components are shown in Fig. 3.

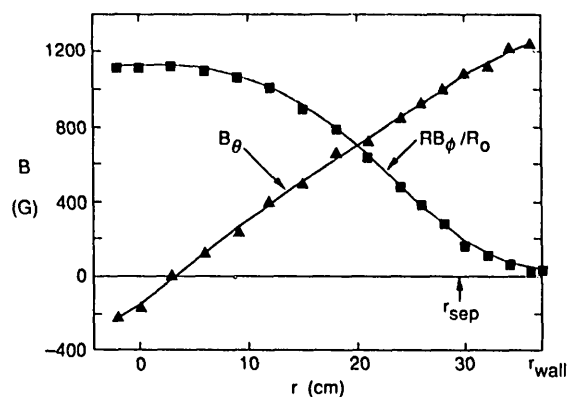


FIG. 3. Profiles of the measured toroidal (B_ϕ) and poloidal (B_θ) components of the equilibrium magnetic field on the device midplane. The wall radius is $r_{\text{wall}} = 37$ cm, and the theoretical radius of the separatrix is $r_{\text{sep}} = 29.5 \pm 1.0$ cm.

LETTERS

The theoretical location of the magnetic separatrix, estimated from numerical equilibrium calculations, is indicated. The radial (horizontal) component was small ($B_r \leq 20$ G), indicating a vertically centred plasma, and the magnetic axis was shifted outward ~ 3 cm from the geometric axis. Rise of the poloidal field out to the wall is expected, resulting from the poloidal flux compression caused by the wall indentations on the midplane.

The on-axis toroidal loop voltage at peak plasma current,

$$V_{\text{loop}} = 2\pi R_0 E_{\phi_0} \approx V_{\text{pg}} - \alpha d\Phi_r/dt \quad (1)$$

was ~ 136 V. V_{pg} is the poloidal gap voltage, and $\alpha d\Phi_r/dt \approx 13$ V represents the inductive voltage due to the portion α of the total ring generated flux, Φ_r , which links the plasma. If a simple Ohm's law applies, then, on axis, $E_{\phi_0} = \eta_0 J_{\phi_0}$. Assuming cylindrical symmetry near the axis,

$$\mu_0 J_{\phi_0} = (\nabla \times \vec{B})_{\phi, r=0} = \frac{1}{r} \frac{\partial}{\partial r} (rB_{\theta})_{r=0} \quad (2)$$

and a measurement of η_0 is possible. When η_0 was compared with the Spitzer resistivity [13] given by the measured electron temperature for $Z = 1$, it was found that $\eta_0/\eta_{\text{Spitzer}} \sim 12$. No measurement of the effective charge state Z_{eff} was made, but the value required to produce a classical resistivity is large, and it may be that non-classical effects, for example fluctuations or field errors, enhanced the loop voltage.

3. CHARACTERISTICS OF AN OBSERVED ASYMMETRY

Despite the well behaved appearance of the quantities shown in Fig. 2, local measurements of the magnetic field uncovered a large, stationary asymmetry which set in at about the time of toroidal field reversal at the wall. Seven probes, as described in Section 2, were distributed toroidally around the device and located near the wall on the midplane to check toroidal symmetry. The measurements of the toroidal and poloidal components of the magnetic field for a typical plasma are plotted in Fig. 4. The magnitude of the magnetic perturbation was $\delta B/B \sim 40\%$. This asymmetry was always observed, and it was probably

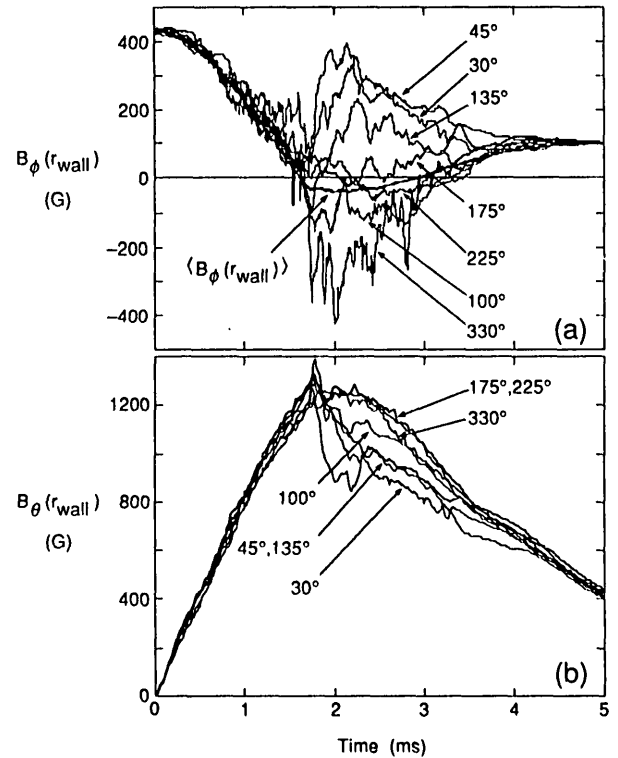


FIG. 4. Plots of the time evolution of (a) the toroidal component and (b) the poloidal component of the midplane magnetic field measured 2.0 cm from the wall surface at seven toroidal azimuths. $\langle B_{\phi}(r_{\text{wall}}) \rangle$ is the spatially averaged toroidal field at the wall calculated from the total wall current. The azimuth at which each signal was measured is indicated.

phase locked to a field error since manipulation of the rather large (order of equilibrium field) poloidal gap field error could alter the locked phase. Since this behaviour was not observed in ultra-low- q divertor discharges ($q_{\text{edge}} \sim 0.3$) or in non-circular RFP discharges produced in this device (without the divertor rings) with similar field errors [14], the asymmetry was probably not initiated by field errors but more likely resulted from instability.

The poloidal mode structure of the asymmetry was dominated by the poloidal mode number $m = 1$. To illustrate this, midplane radial profiles of the radial magnetic field B_r , measured at $\phi = 135^\circ$ and $\phi = 225^\circ$, are plotted in Fig. 5. The data points are B_r , time averaged from 2.5 to 3.0 ms, measured for shots in which the asymmetry was nearly identical, as determined by matching signals from stationary probes placed near the wall. These particular shots should represent the profiles that would be measured in a single, typical plasma. The large axis value of B_r identifies a large $m = 1$ component. The transverse

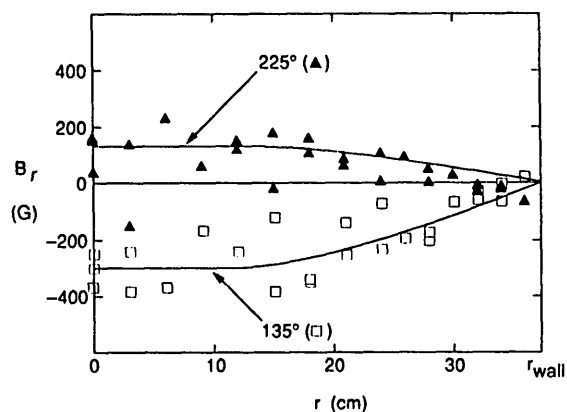


FIG. 5. Measurements of the radial (horizontal) component of the midplane magnetic field at $\phi = 135^\circ$ and $\phi = 225^\circ$.

magnetic signals from a set of six probes located near the wall at $\phi = 225^\circ$ but separated poloidally exhibited a dominant $m = 1$ dependence, although the $m = 2$ and $m = 3$ amplitudes were only $\sim 50\%$ smaller. The non-circular vacuum vessel wall, however, distorts the perturbation generated by internal $m = 1$ plasma motion, and larger mode numbers are expected to be detected near the wall. It is likely that $m > 1$ modes were small internally.

The toroidal mode structure was more complicated. Presuming a single mode, phase measurements using the signals from closely spaced probes on the midplane, such as those at $\phi = 30^\circ$, $\phi = 45^\circ$ and $\phi = 330^\circ$ shown in Fig. 4, suggest a toroidal mode number $|n| \approx 4-6$, but the signals at all locations do not, in general, fit a single mode. Unfortunately, there were too few measurements to perform a proper Fourier analysis if mode numbers $|n| \geq 4$ were present. From the equilibrium field profiles measured just before the onset of the asymmetry, the axis safety factor was $q_0 = 0.19 \pm 0.01$, so modes with $m = 1$, $-n \geq 6$, would have been internally resonant.

Although little is known about the magnitude of the toroidal mode numbers, the sense of the pitch of the modes can be inferred from the relationship

$$\begin{aligned} \tilde{B}_\theta \left(r = r_{\text{wall}}, \theta = \text{midplane}, \phi \right) \\ = \frac{m}{n} \frac{R_{\text{wall}}}{r_{\text{wall}}} \tilde{B}_\phi \left(r = r_{\text{wall}}, \theta = \text{midplane}, \phi \right) \end{aligned} \quad (3)$$

resulting from the boundary condition that the normal component of the perturbed current density

vanish at the conducting wall. Equation (3) was derived for locations on the midplane for the case of a single mode using Ampere's law to relate the perturbed current density to the perturbed magnetic field \tilde{B} . The equation implies that measurements of $\tilde{B}_{\theta \text{ wall}}$ and $\tilde{B}_{\phi \text{ wall}}$ at any toroidal azimuth would lie on a line with a slope proportional to m/n when plotted as $\tilde{B}_{\theta \text{ wall}}$ versus $\tilde{B}_{\phi \text{ wall}}$. A negative slope ($n < 0$) indicates that the mode pitch is in the same sense as the equilibrium field near the axis. For the case of several equally sized modes, the linear relationship between $\tilde{B}_{\theta \text{ wall}}$ and $\tilde{B}_{\phi \text{ wall}}$ is destroyed. However, if the modes are closely spaced in m and n , the points $\tilde{B}_{\theta \text{ wall}}$ versus $\tilde{B}_{\phi \text{ wall}}$ at all toroidal azimuths differ only slightly from the single-mode linear relationship, and the sense of the pitch for these similar modes can still be inferred.

In the experiment, all the measurements of $\tilde{B}_{\theta \text{ wall}}$ versus $\tilde{B}_{\phi \text{ wall}}$ were nearly linearly related. This is illustrated in Fig. 6, where $B_{\theta \text{ wall}}$ and $B_{\phi \text{ wall}}$, time averaged over a $300 \mu\text{s}$ interval during the period of the asymmetry, are plotted for two plasmas with different locked phases of the asymmetry. (Plotting the total fields $B_{\theta \text{ wall}}$ and $B_{\phi \text{ wall}}$ simply adds an offset equal to the symmetric portion of the field.) Any line that reasonably fits the data in Fig. 6 has a negative slope, indicating that the dominant mode – or band of modes – was internally resonant or internally non-resonant. In addition, when the locked phase changed, the points $B_{\theta \text{ wall}}$ versus $B_{\phi \text{ wall}}$ moved along the same line.

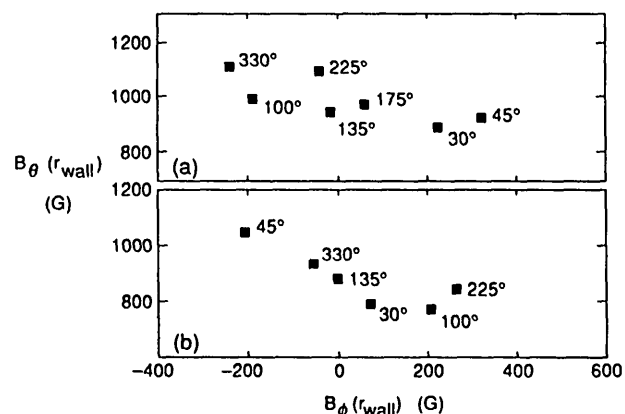


FIG. 6. Plots of the poloidal component versus the toroidal component of the midplane magnetic field near the wall, time averaged from 2.4 ms to 2.7 ms, for (a) the most often occurring locked phase of the asymmetry and (b) a different locked phase. The toroidal azimuth at which each measurement was taken is indicated.

4. DISCUSSION

The large, stationary asymmetry observed in the poloidal divertor plasma might be the result of an unstable, non-reversed equilibrium. The asymmetry was observed to set in at about the time when the toroidal magnetic field reversed at the wall, but, at this time, the toroidal field was somewhat more positive at the separatrix (implying that the separatrix was not a perfect current limiter). This asymmetry is best described by the mode numbers $m = 1$ and $n \sim -5$. Although the poloidal divertor configuration is highly non-circular, linear [7] and non-linear [8] MHD stability calculations of a cylindrical plasma far from the stabilizing wall should serve as a guide to predict the types of instability expected for the analogous poloidal divertor equilibria. Internally resonant and non-resonant $m = 1$ modes are predicted to be unstable for cylindrical non-reversed equilibria when the stabilizing wall is distant. Moreover, the most unstable modes are those non-resonant or resonant near the axis. If this holds true in the poloidal divertor configuration, then the most unstable mode at the time when the asymmetry struck the plasma would have been $m = 1$, $n = -5$.

Circular RFP plasmas bounded by a relatively thin vacuum layer exhibit large fluctuation amplitudes during the non-reversed setup phase, but the fluctuations do not prevent the formation of relatively quiescent, symmetric RFP equilibria. In the poloidal divertor experiment, the large vacuum region probably leads to a relatively large range of unstable equilibria and to increased growth rates and non-linearly saturated amplitudes of the unstable modes. The failure of the poloidal divertor plasma to obtain a quiescent, RFP-like equilibrium may be due to excessively large perturbations generated late in the setup phase. Without an equivalent stability analysis or a simulation including the poloidal divertor geometry, the details of the MHD stability of the poloidal divertor configuration remain uncertain.

ACKNOWLEDGEMENTS

The authors wish to thank J. Laufenberg and T. Lovell for their technical assistance and Y.L. Ho for providing the numerical equilibrium calculations and for useful discussions.

This work was supported by the United States Department of Energy.

REFERENCES

- [1] BODIN, H.A.B., NEWTON, A.A., Nucl. Fusion **20** (1980) 1255.
- [2] ROBINSON, D.C., Plasma Phys. **13** (1971) 439.
- [3] ROBINSON, D.C., Nucl. Fusion **18** (1978) 939.
- [4] GOFORTH, R.R., CARLSTROM, T.N., CHU, C., et al., Nucl. Fusion **26** (1986) 515.
- [5] ASAKURA, N., FUJISAWA, A., FUJITA, T., et al., in Plasma Physics and Controlled Nuclear Fusion Research 1986 (Proc. 11th Int. Conf. Kyoto, 1986), Vol. 2, IAEA, Vienna (1987) 433.
- [6] ROBERTSON, S., SCHMID, P., Phys. Fluids **30** (1987) 884.
- [7] HO, Y.L., PRAGER, S.C., Phys. Fluids **31** (1988) 1673.
- [8] HO, Y.L., PRAGER, S.C., SCHNACK, D.D., Nonlinear behaviour of the reversed field pinch with nonideal boundary conditions, submitted to Phys. Rev. Lett.
- [9] DEXTER, R.N., KERST, D.W., LOVELL, T.W., PRAGER, S.C., SPROTT, J.C., Bull. Am. Phys. Soc. **29** (1984) 1332.
- [10] SARFF, J.S., TURNER, L., SPROTT, J.C., Phys. Fluids **30** (1987) 2155.
- [11] La HAYE, R.J., CARLSTROM, T.N., GOFORTH, R.R., JACKSON, G.L., SCHAFFER, M.J., TAMANO, T., TAYLOR, P.L., Phys. Fluids **27** (1984) 2576.
- [12] La HAYE, R.J., JENSEN, T.H., LEE, P.S.C., MOORE, R.W., OHKAWA, T., Nucl. Fusion **26** (1986) 255.
- [13] SPITZER, L., Jr., HARM, R., Phys. Rev. **89** (1953) 977.
- [14] ALMAGRI, A., ASSADI, S., DEXTER, R.N., PRAGER, S.C., SARFF, J.S., SPROTT, J.C., Nucl. Fusion **27** (1987) 1795.

(Manuscript received 15 July 1988)

Final manuscript received 10 October 1988)